



Energy flow of electric dipole radiation in between parallel mirrors

Zhangjin Xu and Henk F. Arnoldus

Department of Physics and Astronomy, Mississippi State University, Mississippi State, MS, USA

ABSTRACT

We have studied the energy flow patterns of the radiation emitted by an electric dipole located in between parallel mirrors. It appears that the field lines of the Poynting vector (the flow lines of energy) can have very intricate structures, including many singularities and vortices. The flow line patterns depend on the distance between the mirrors, the distance of the dipole to one of the mirrors and the angle of oscillation of the dipole moment with respect to the normal of the mirror surfaces. Already for the simplest case of a dipole moment oscillating perpendicular to the mirrors, singularities appear at regular intervals along the direction of propagation (parallel to the mirrors). For a parallel dipole, vortices appear in the neighbourhood of the dipole. For a dipole oscillating under a finite angle with the surface normal, the radiating tends to swirl around the dipole before travelling off parallel to the mirrors. For relatively large mirror separations, vortices appear in the pattern. When the dipole is off-centred with respect to the midway point between the mirrors, the flow line structure becomes even more complicated, with numerous vortices in the pattern, and tiny loops near the dipole. We have also investigated the locations of the vortices and singularities, and these can be found without any specific knowledge about the flow lines. This provides an independent means of studying the propagation of dipole radiation between mirrors.

ARTICLE HISTORY

Received 26 February 2017
Accepted 10 June 2017

KEYWORDS

Electric dipole; Poynting vector; optical vortex

1. Introduction

An atom or molecule in an excited electronic state will decay spontaneously to the ground state, and at the same time a fluorescent photon is emitted. Assuming a steady excitation of the particle, for instance by a laser beam, this leads to a steady emission of photons. The emission rate, multiplied by the energy of a photon, is the emitted power, and the inverse of the emission rate is the lifetime of the excited state. We shall assume that the particle can be represented by an oscillating electric dipole moment. When the particle is located close to an interface with a dielectric material or a mirror, the photon emission rate is altered due to the fact that the reflected radiation partially travels back to the particle and the reflected electric field at the location of the dipole alters the emission rate (1). Of particular interest is the dependence of the emission rate on the distance between the dipole and the interface. The dependence of the emission rate on the various parameters has been studied by numerous authors, both theoretically and experimentally (2–10). Also of interest is the modification of the far-field radiation pattern, as it is modified by interference between directly emitted and reflected light (11, 12). An obvious generalization of the

case of a dipole near an interface is the situation where the emitter is located in between two parallel interfaces (13–18). When the two interfaces are mirrors, a relatively simple expression can be derived for the emission rate. It follows theoretically that spontaneous emission is ‘turned off’ entirely when the distance between the mirrors is less than half a wavelength of the radiation, and when the dipole moment is oriented parallel to the mirror surfaces. This has been observed experimentally for Rydberg atoms in between parallel mirrors (19).

When a small particle emits radiation near an interface, the presence of the interface alters the decay rate due to reflected radiation which comes back to the particle. A simultaneous phenomenon is that the reflected light and the direct light interfere, and this is responsible for constructive and destructive interference, leading to lobes in the power per unit solid angle in the far field. In the near field, however, this interference leads to complicated energy flow patterns in the neighbourhood of the particle. For a single mirror, numerous singularities and vortices appear (20) and the flow lines of energy are far from trivial. From a larger view, it appears that four strings containing small vortices appear to come out of the location

CONTACT Henk F. Arnoldus  hfa1@msstate.edu

This article was originally published with errors. This version has been corrected. Please see Erratum (<http://dx.doi.org/10.1080/09500340.2017.1349263>).

© 2017 Informa UK Limited, trading as Taylor & Francis Group

of the dipole (21). An interesting phenomenon occurs when dipole radiation passes through an interface with a dielectric (22, 23). When the medium is thicker than the embedding medium of the dipole, radiation passes through more or less in straight lines, similar to optical rays. When the medium is thinner, however, some radiation that transmits into the medium turns around and passes through the interface again. Then, it turns around again and so on. This leads to an oscillating energy flow back and forth through the interface, and at each crossing a vortex appears.

2. Dipole in between mirrors

We shall consider an electric dipole located in between parallel mirrors, as shown in Figure 1. The dipole is located on the z axis, a distance H above the lower mirror. The surface of the lower mirror is the xy plane and the surface of the second mirror is the $z = D$ plane. The dipole moment $\mathbf{d}(t)$ oscillates harmonically with angular frequency ω :

$$\mathbf{d}(t) = \text{Re}(\mathbf{d}e^{-i\omega t}), \quad (1)$$

with \mathbf{d} the complex amplitude. We set

$$\mathbf{d} = d_0 \hat{\mathbf{u}}_0, \quad d_0 > 0, \quad \hat{\mathbf{u}}_0 \cdot \hat{\mathbf{u}}_0^* = 1, \quad (2)$$

and here the unit polarization vector $\hat{\mathbf{u}}_0$ may be complex (as for circular or elliptical polarization). The electric field $\mathbf{E}(\mathbf{r}, t)$ in between the mirrors is

$$\mathbf{E}(\mathbf{r}, t) = \text{Re}[\mathbf{E}(\mathbf{r})e^{-i\omega t}], \quad (3)$$

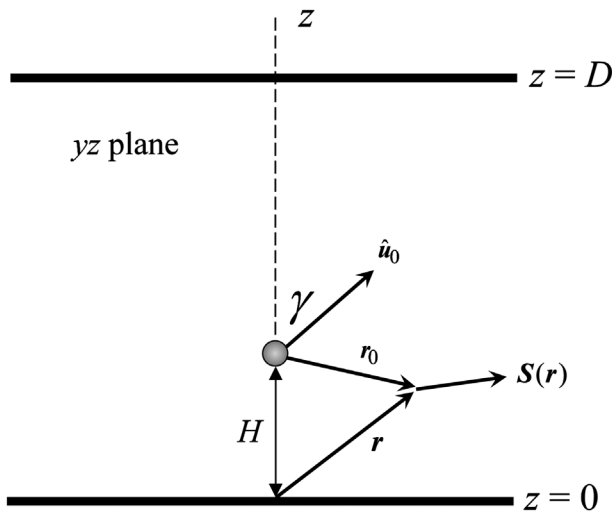


Figure 1. The dipole is located on the z axis, a distance H above the lower mirror. The vector \mathbf{r}_0 represents the field point \mathbf{r} , but measured from the location of the dipole. The Poynting vector at the field point is indicated by vector $\mathbf{S}(\mathbf{r})$. For a linear dipole, oscillating in the yz plane, the unit vector $\hat{\mathbf{u}}_0$ makes an angle γ with the positive z axis.

with $\mathbf{E}(\mathbf{r})$ the complex amplitude and the magnetic field $\mathbf{B}(\mathbf{r}, t)$ is expressed similarly. Here, \mathbf{r} is the position vector of the field point of interest. For the radiation emitted by the dipole, it is convenient to introduce the position vector of the field point with respect to the location of the dipole as follows:

$$\mathbf{r}_0 = \mathbf{r} - H\mathbf{e}_z, \quad (4)$$

and this vector is shown in Figure 1. With the help of the wave number $k = \omega/c$, we introduce dimensionless variables. The dimensionless position vector of the field point is $\mathbf{q} = k\mathbf{r}$ and similarly $\mathbf{q}_0 = k\mathbf{r}_0$. The dimensionless complex amplitudes $\mathbf{e}(\mathbf{r})$ and $\mathbf{b}(\mathbf{r})$ of the electric and magnetic fields, respectively, are defined as follows:

$$\mathbf{E}(\mathbf{r}) = \zeta \mathbf{e}(\mathbf{r}), \quad (5)$$

$$\mathbf{B}(\mathbf{r}) = \frac{\zeta}{c} \mathbf{b}(\mathbf{r}), \quad (6)$$

with

$$\zeta = \frac{k^3 d_0}{4\pi\epsilon_0}. \quad (7)$$

For the fields emitted by the dipole we then have (24)

$$\mathbf{e}_0(\mathbf{r}) = \left\{ \hat{\mathbf{u}}_0 - (\hat{\mathbf{q}}_0 \cdot \hat{\mathbf{u}}_0) \hat{\mathbf{q}}_0 + [\hat{\mathbf{u}}_0 - 3(\hat{\mathbf{q}}_0 \cdot \hat{\mathbf{u}}_0) \hat{\mathbf{q}}_0] \frac{i}{q_0} \left(1 + \frac{i}{q_0} \right) \right\} \frac{e^{iq_0}}{q_0}, \quad (8)$$

$$\mathbf{b}_0(\mathbf{r}) = (\hat{\mathbf{q}}_0 \times \hat{\mathbf{u}}_0) \left(1 + \frac{i}{q_0} \right) \frac{e^{iq_0}}{q_0}. \quad (9)$$

The subscripts '0' everywhere are for later purpose.

3. The image system

The radiation emitted by the dipole bounces off the mirrors and multiple reflections lead to complicated interference patterns. This system can be analysed most easily with the method of images. In between the mirrors, the dipole field is a solution of Maxwell equations. At the mirror surfaces we must have that the parallel component of the electric field vanishes and the perpendicular component of the magnetic field must be zero. To this end, mirror images are introduced outside the region $0 < z < D$, such that the total fields at the mirror surfaces satisfy the boundary conditions. For a single (bottom) mirror, this image is located at a distance H below the mirror and its dipole moment has its parallel component reversed. So if we write

$$\hat{\mathbf{u}}_0 = (\hat{\mathbf{u}}_0)_\perp + (\hat{\mathbf{u}}_0)_\parallel, \quad (10)$$

then the mirror dipole has polarization vector

$$\hat{\mathbf{u}}_0^{\text{mi}} = (\hat{\mathbf{u}}_0)_\perp - (\hat{\mathbf{u}}_0)_\parallel. \quad (11)$$

It can then be verified that the total fields satisfy the boundary conditions.

For the case of two mirrors, the dipole has an image in both mirrors. But then, the image of the dipole in the lower mirror produces a field at the position of the upper mirror. Therefore, we need an image of the first image with respect to the upper mirror to compensate for this. This continues indefinitely, leading to an infinite array of images on the z axis. We shall number the images with m , and such that above the top mirror we have $m > 0$ and below the bottom mirror we have $m < 0$. The value $m = 0$ is taken to correspond to the dipole itself. It then follows by inspection that the m th image is located at

$$z_m = \left(m + \frac{1}{2}\right)D + (-1)^m \left(H - \frac{1}{2}D\right). \quad (12)$$

The location of the images is illustrated in Figure 2. Equation (12) can be written as follows:

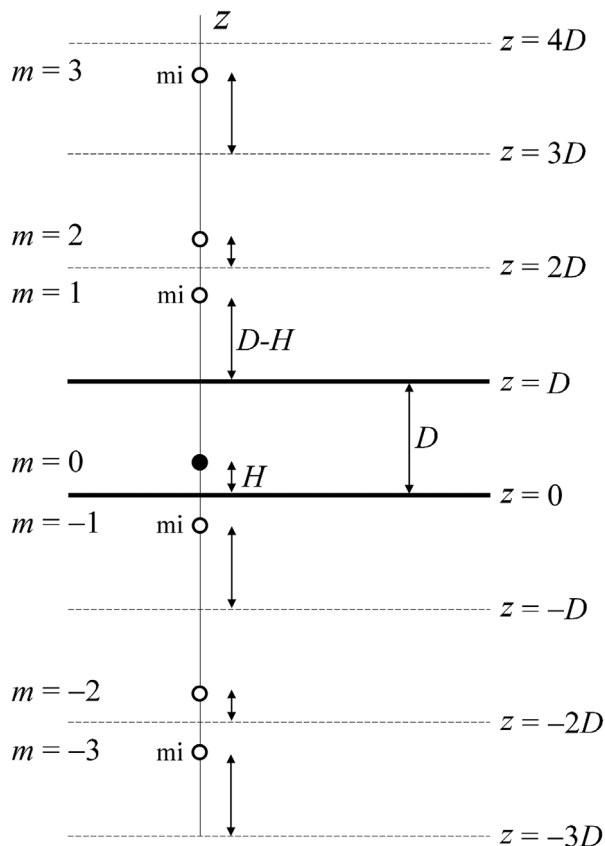


Figure 2. The diagram shows the locations of the mirror images.

$$z_m = \begin{cases} mD + H, & m \text{ even} \\ (m+1)D - H, & m \text{ odd} \end{cases}, \quad (13)$$

and this shows that the m th image is located in between the planes $z = mD$ and $z = (m+1)D$. We also see that images with m even have polarization vector $\hat{\mathbf{u}}_0$ and images with m odd have $\hat{\mathbf{u}}_0^{\text{mi}}$ as polarization vector. This can be combined as follows:

$$\hat{\mathbf{u}}_m = (\hat{\mathbf{u}}_0)_\perp + (-1)^m (\hat{\mathbf{u}}_0)_\parallel, \quad (14)$$

for the polarization vector of the m th image.

4. Fields and Poynting vector

Each image dipole radiates an electric and magnetic field, similar to Equations (8) and (9) for the dipole. For the fields by the m th image, we replace $\hat{\mathbf{u}}_0$ by $\hat{\mathbf{u}}_m$ from Equation (14) and the dimensionless position vector \mathbf{q}_0 of the field point is replaced by

$$\mathbf{q}_m = \mathbf{q} - \bar{z}_m \mathbf{e}_z, \quad (15)$$

with $\bar{z}_m = kz_m$. The dimensionless electric and magnetic fields are $\mathbf{e}_m(\mathbf{r})$ and $\mathbf{b}_m(\mathbf{r})$, respectively, and the total fields at field point \mathbf{r} are

$$\mathbf{e}(\mathbf{r}) = \sum_{m=-\infty}^{\infty} \mathbf{e}_m(\mathbf{r}), \quad (16)$$

$$\mathbf{b}(\mathbf{r}) = \sum_{m=-\infty}^{\infty} \mathbf{b}_m(\mathbf{r}). \quad (17)$$

Energy in between the mirrors flows along the field lines of the Poynting vector $\mathbf{S}(\mathbf{r}, t)$. For time-harmonic fields, we consider the time-averaged Poynting vector:

$$\mathbf{S}(\mathbf{r}) = \frac{1}{2\mu_0} \text{Re}[\mathbf{E}(\mathbf{r}) \times \mathbf{B}(\mathbf{r})^*], \quad (18)$$

which is time-independent. We split off a factor

$$\mathbf{S}(\mathbf{r}) = \frac{\zeta^2}{2\mu_0 c} \boldsymbol{\sigma}(\mathbf{r}), \quad (19)$$

so that

$$\boldsymbol{\sigma}(\mathbf{r}) = \text{Re}[\mathbf{e}(\mathbf{r}) \times \mathbf{b}(\mathbf{r})^*]. \quad (20)$$

With $\mathbf{e}(\mathbf{r})$ and $\mathbf{b}(\mathbf{r})$ from Equations (16) and (17) substituted, we see that we get cross-terms between all the m values. Vector $\boldsymbol{\sigma}(\mathbf{r})$ depends only on \mathbf{q} (and not \mathbf{r}), so we shall write $\boldsymbol{\sigma}(\mathbf{q})$.

Equation (20) determines the Poynting vector at a field point \mathbf{q} . Let $\mathbf{q}(u)$ be a parametrization of a field line

through a given initial point $(\bar{x}_0, \bar{y}_0, \bar{z}_0)$, with $\bar{x}_0 = kx_0$, etc. The curves $\mathbf{q}(u)$ are then the solution of

$$\frac{d}{du}\mathbf{q}(u) = f(\mathbf{q})\boldsymbol{\sigma}(\mathbf{q}(u)). \quad (21)$$

Here, $f(\mathbf{q})$ is an arbitrary positive function of \mathbf{q} , which can be selected for convenience or numerical stability. A good choice seems to be $f(\mathbf{q}) = q_0^4$. We use *Mathematica* to solve Equation (21) (which is actually a set of three equations when written out in Cartesian coordinates).

The sums over m in Equations (16) and (17) obviously needs to be truncated with a certain maximum M ($-M \leq m \leq M$, so $2M + 1$ dipoles). This M is determined by considering the Poynting vector near the two mirrors. At a mirror surface, the Poynting vector must be parallel to the surface (no energy flows through the mirrors). Only for a sufficient large value of M will this be the case and we find that values of M of about 100 are usually necessary for convergence.

5. Linear dipole

The field lines of the Poynting vector are in general 3D curves, which makes it very difficult to visualize energy flow line patterns. A great simplification arises if we assume that the dipole oscillates linearly, as in Figure 1. The direction of oscillation is specified by the angle γ with the positive z axis and we take the plane of oscillation as the yz plane. We then have

$$\hat{\mathbf{u}}_0 = \mathbf{e}_z \cos \gamma + \mathbf{e}_y \sin \gamma, \quad (22)$$

and for the images we obtain

$$\hat{\mathbf{u}}_m = \mathbf{e}_z \cos \gamma + (-1)^m \mathbf{e}_y \sin \gamma. \quad (23)$$

Let us now consider a field point in the yz plane. It follows from Equation (8) (with $0 \rightarrow m$) that $\mathbf{e}_m(\mathbf{q})$ is in the yz plane and we see from Equation (9) that $\mathbf{b}_m(\mathbf{q})$ is along the x axis. Therefore, the Poynting vector $\boldsymbol{\sigma}(\mathbf{q})$ is in the yz plane. Consequently, if a field line of the Poynting vector goes through a point in the yz plane, then the entire field line lies in the yz plane. Similarly, it is easy to verify that the field line pattern is reflection symmetric in the yz plane, so we only need to consider field lines in the region $x \geq 0$. The yz plane is a symmetry plane, and field lines in this plane are 2D curves.

6. Vertical dipole

In the graphs to follow, we use dimensionless coordinates $\bar{y} = ky$ and $\bar{z} = kz$ for points in the yz plane and we introduce $\delta = kD$ for the dimensionless distance between the mirrors and $h = kH$ for the dimensionless distance

between the dipole and the lower mirror. We shall first consider the case $\gamma = 0$, corresponding to a dipole oscillating along the z axis, and with the dipole located midway between the mirrors. For a linear dipole in free space, the field lines are straight, coming out of the dipole and running to infinity. We see from Figure 3 that close to the dipole the field lines indeed come out of the dipole, and almost as straight lines. At this close distance it seems that the mirrors have no effect yet. When the field lines approach the mirrors, they bend and then run off to infinity. For $\gamma = 0$, the system is rotation symmetric around the \bar{z} axis, so there are no additional features off the $\bar{y}\bar{z}$ plane.

The flow lines in Figure 3 are what one would expect for the energy flow in between mirrors when the flow lines come out of the dipole. Figure 4 shows an extension to the right of the flow pattern in Figure 3. We see that, instead of smoothly running off to infinity, two singularities appear near the midway plane between the mirrors. At a singularity, the Poynting vector vanishes and such singularities are indicated by small circles. Figure 5 shows a further extension of the graph, and now we notice that two singularities appear close to the mirror surfaces. Since for a vertical dipole the field line picture is rotation symmetric around the \bar{z} axis, these singularities are singular circles around the \bar{z} axis. We have verified numerically that this picture continues to the right indefinitely. After about 8 units further, two singularities appear along the midway plane, then again 8 units further two near the mirrors and so on.

The pattern with the sequences of singularities in Figures 3–5 seems to be universal for a vertical dipole located at the midway point. The locations of the singularities, in the horizontal direction, depend on δ . The larger the separation between the mirrors, the further apart the singularities are. However, it seems that there are always two singularities near the midway plane and two singularities near the mirrors. The number of singularities does not seem to increase with the mirror separation. When the mirror separation is less than about $\delta = \pi$, there are no singularities, and the radiation flows along almost straight lines to infinity. Since 2π corresponds to an optical wavelength, we conclude that the mirror separation must be at least half a wavelength for the singular circles in the flow pattern to appear.

7. Horizontal dipole

We now consider a horizontal dipole ($\gamma = \pi/2$) located midway between the mirrors. Figure 6 shows the energy flow picture for $\delta = 4$. Energy is emitted by the dipole in the up and down directions and the flow lines bend at the mirror surfaces, just like in Figure 3. For a dipole in free space, no energy is emitted along the dipole axis and the

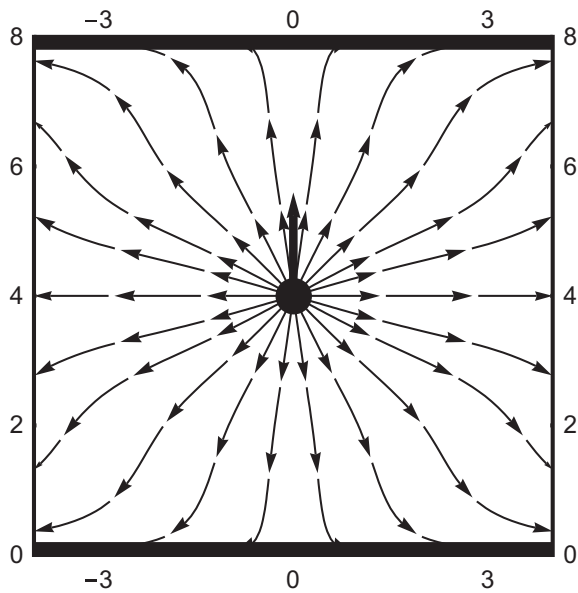


Figure 3. The figure shows field lines of the Poynting vector in the $\bar{y}\bar{z}$ plane for a vertical dipole. In this and other figures, we shall take \bar{z} as up and \bar{y} to the right. The dipole moment vector \hat{u}_0 is represented by an arrow (not to scale). The distance between the mirrors is $\delta = 8$ and the locations of the mirrors are indicated by fat black lines. The dipole is located midway between the mirrors, so at $h = 4$.

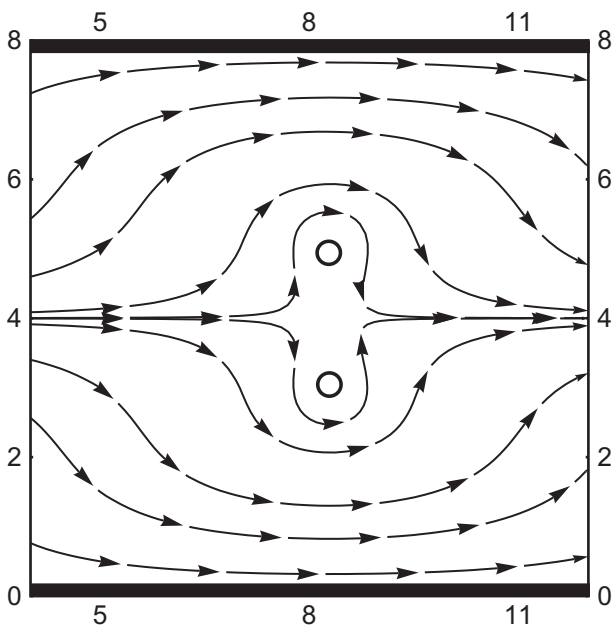


Figure 4. This figure is an extension to the right of Figure 3. The white circles are singularities.

same appears to hold here. The line $\bar{z} = 2$ is a singular line, with no energy flow along this line (indicated by a dashed line in the figure). Radiation emitted upward and downward changes direction at the mirror surfaces, after which

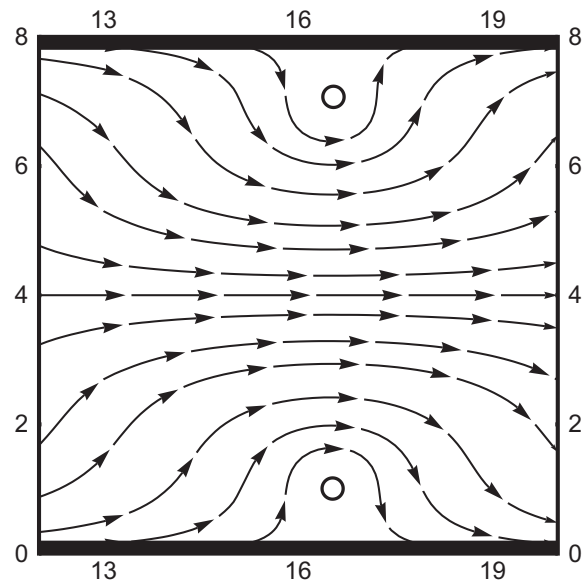


Figure 5. This figure is an extension to the right of Figure 4.

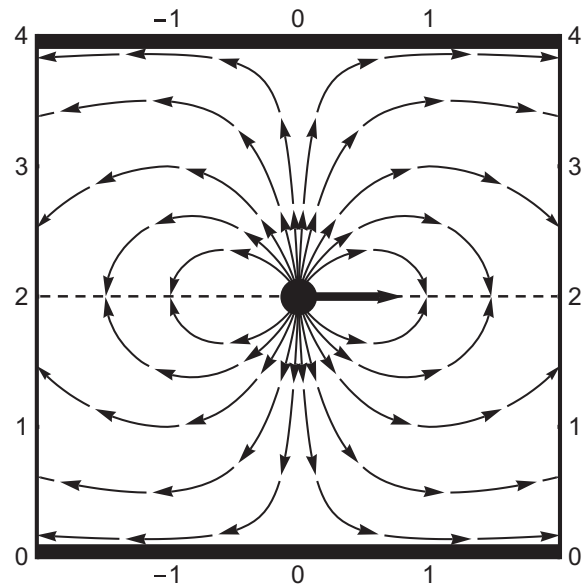


Figure 6. Shown are the field lines of energy flow for a horizontal dipole midway between the mirrors, for $\delta = 4$.

the flow lines bend to the dipole axis $\bar{z} = 2$ and the flow lines end at this axis. For a dipole in free space, the field lines are straight, but due to the presence of the mirrors here, all field lines bend to the dipole axis and end there. This is also clear from Figure 7, which is an extension to the right of Figure 6.

When the distance between the mirrors is increased, four vortices appear near the location of the dipole. This is shown in Figure 8. Not all field lines end at the dipole axis, as for smaller δ . Close to the dipole, field lines start at the dipole axis and then swirl into the vortices, where

they end. Further out, the field lines again bend towards the axis, as in Figure 7. In the transition region, there are two singularities on the dipole axis, which are indicated by white circles in the figure. For even larger δ , a similar structure as in Figures 4 and 5 appears, where there are sets of singularities alternating in location.

8. Dipole under an angle

We now consider the effect of an angle γ between the \bar{z} axis and the direction of oscillation \hat{u}_0 of the dipole. A

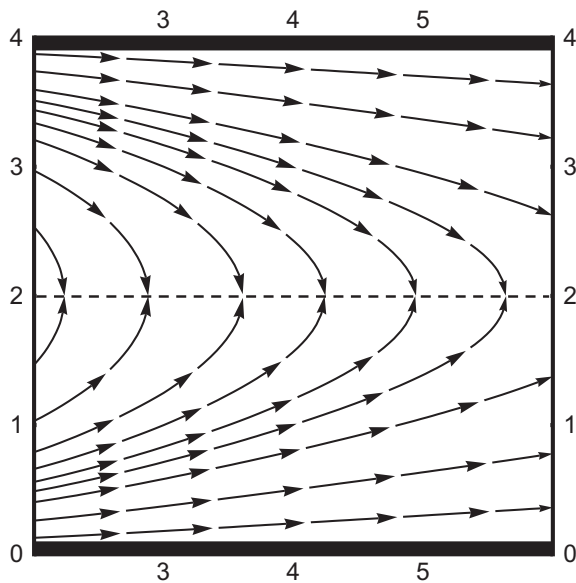


Figure 7. This figure is an extension to the right of Figure 6.

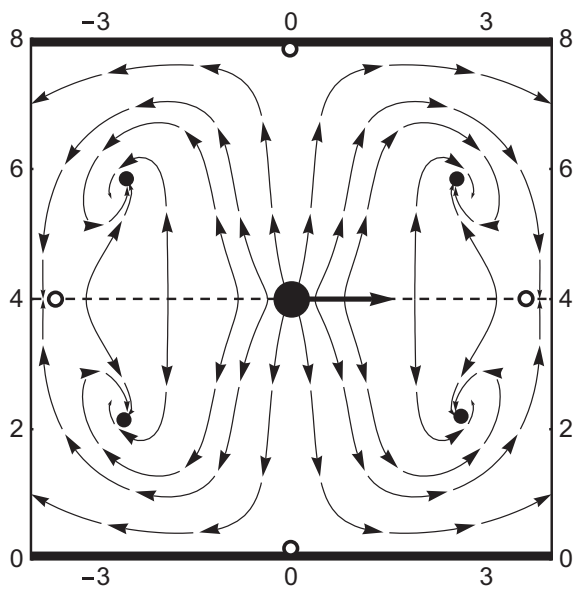


Figure 8. The figure shows the energy flow lines for $\delta = 8$, $h = 4$ and $\gamma = \pi/2$. The black circles are at the centres of vortices and the white circles are other singularities.

typical flow line pattern for small δ is shown in Figure 9. Most of the radiation is emitted perpendicular to the dipole axis, as in free space. We see that field lines coming out of the dipole swing around the dipole and then run off to infinity. Some field lines make half a swing, as for curve *a*, and some make a full swing, as for curve *b*. For larger values of the mirror separation, vortices appear along the dipole axis. This is illustrated in Figure 10. Two large vortices form in the top-right and the bottom-left of the picture, and in between the large vortices and the dipole two small vortices appear. An enlargement of the top-right vortices is shown in Figure 11. When we increase δ even further, more vortices appear approximately along the dipole axis.

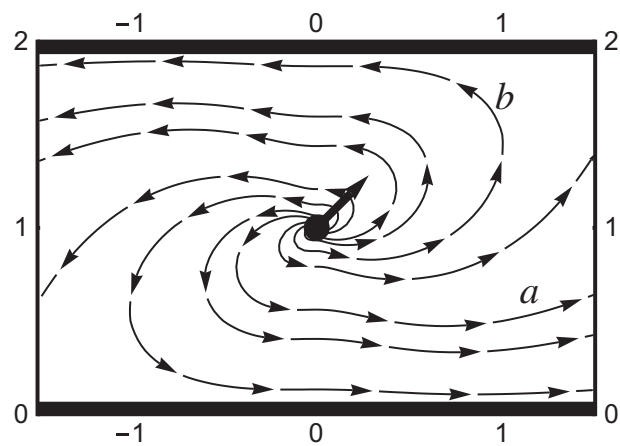


Figure 9. The dipole oscillates under 45° with the \bar{z} axis, and we have $\delta = 2$.

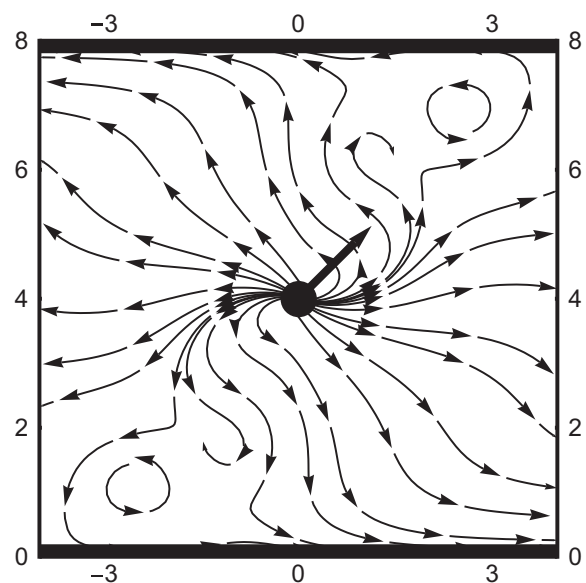


Figure 10. Field lines for a dipole oscillating under 45° with the \bar{z} axis, and for $\delta = 8$.

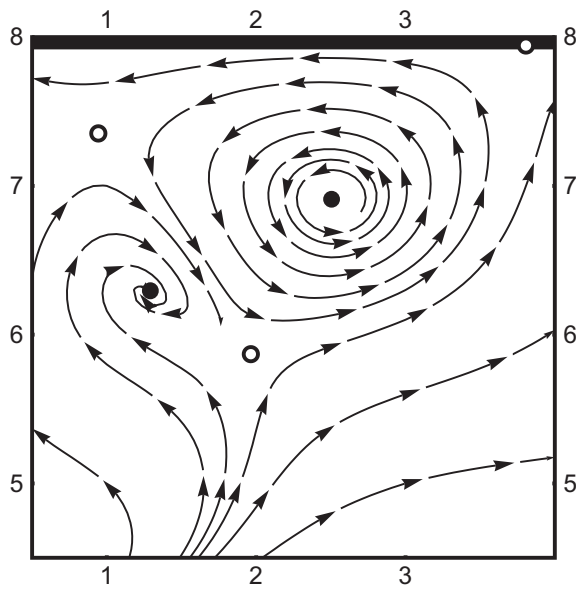


Figure 11. The figure shows an enlargement of the top-right vortex in Figure 10. The black circles are at the centres of the vortices and the white circles are other singularities.

9. Energy flow near a vortex

The energy flow lines near the small vortex in Figure 11 end at the centre of the vortex and the flow line (only one shown) near the large vortex comes out of the centre of the vortex and then runs off to the left. At the centre of each vortex is a singularity, indicated by small circles, and three more singularities can be seen in the picture. It seems that the small vortex is an energy sink and the large vortex is an energy source. Since the flow line pattern is time independent, this can obviously not be the case. Energy cannot pile up at the centre of the small vortex, and no energy is created at the centre of the large vortex. From a mathematical point of view, the divergence of the Poynting vector is zero in between the mirrors, except at the location of the dipole. There are no energy sinks or sources other than the dipole.

We only draw field lines in the symmetry plane in order to avoid cumbersome 3D visualizations. This gives a good impression of the behaviour of the energy flow in most cases. However, the field line patterns shown are part of larger, 3D pictures. This becomes most relevant when considering the energy flow near a vortex. Figure 12 shows a 3D field line in the neighbourhood of the large vortex in Figure 11. The field line's initial point is taken as $(\bar{x}_0, \bar{y}_0, \bar{z}_0) = (0.02, 3, 7)$, so slightly in front of the $\bar{y}\bar{z}$ plane. The field line is spiralling counterclockwise and it approaches the $\bar{y}\bar{z}$ plane. The spiral gets thinner on approach and then flattens out when reaching the $\bar{y}\bar{z}$ plane. Close to the $\bar{y}\bar{z}$ plane, the field line keeps on spiralling almost parallel to the $\bar{y}\bar{z}$ plane and then it runs off to the left, as in Figure 11. The large spiral in Figure

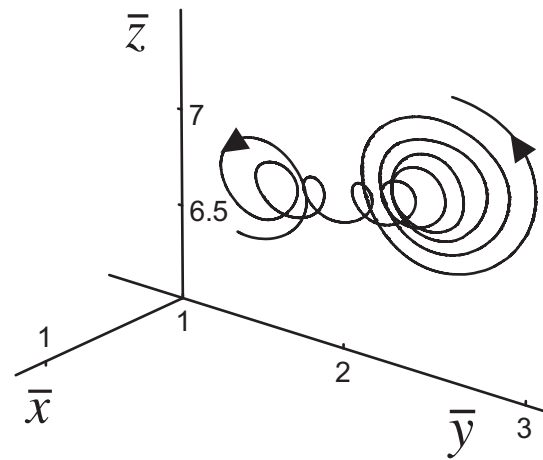


Figure 12. Shown is a 3D field line in the neighbourhood of the large vortex in Figure 11. The axes origin has been moved for clarity of perspective.

12 is almost the same as the spiral in Figure 11. The field line has to flatten out on approach of the $\bar{y}\bar{z}$ plane, since no field line can cross the symmetry plane. The field line pattern is reflection symmetric in the symmetry plane, so a mirror image spiral is present in the region $\bar{x} < 0$. This spiral has the same rotation direction, when viewed down the positive \bar{x} axis. Very close to the $\bar{y}\bar{z}$ plane, both spirals are almost identical to the big spiral in Figure 11. It is clear that neither field line comes out of the singularity at the centre of the 2D vortex. Only for a field line exactly in the $\bar{y}\bar{z}$ plane does the vortex seem to have a source.

10. Dipole off-centre

A new aspect of the energy flow pattern appears when we consider a dipole located off the midway plane between the mirrors. Figure 13 shows field lines for $\delta = 4$, $h = 1$ and $\gamma = \pi/3$. We see that all field lines come out of the dipole at the bottom-right, and some loop around the dipole, and enter the dipole at the other side. Just above the point of entry there is necessarily a singularity. The same phenomenon occurs for a single mirror (20), although under different conditions. A detailed analysis of this exotic effect will be presented elsewhere.

Figure 14 shows the field line pattern for $\delta = 4\pi$, $h = \pi/2$ and $\gamma = \pi/2$. For $\gamma = \pi/2$ the pattern is reflection symmetric in the \bar{z} axis, so only the region $\bar{y} \geq 0$ is shown. We notice the appearance of a large number of vortices. The field lines in the four vortices on the left rotate clockwise and the field lines in the vortices on the right rotate counterclockwise. This pattern repeats if we extend the graph to the right (not shown). Interestingly, if we replace $\delta = 4\pi$ by, say, $\delta = 12$, the entire pattern washes out, and we just get some wiggly curves going to the right. Similarly, if we would replace $\delta = 4$ in Figure 13 by $\delta = \pi$, a vortex appears

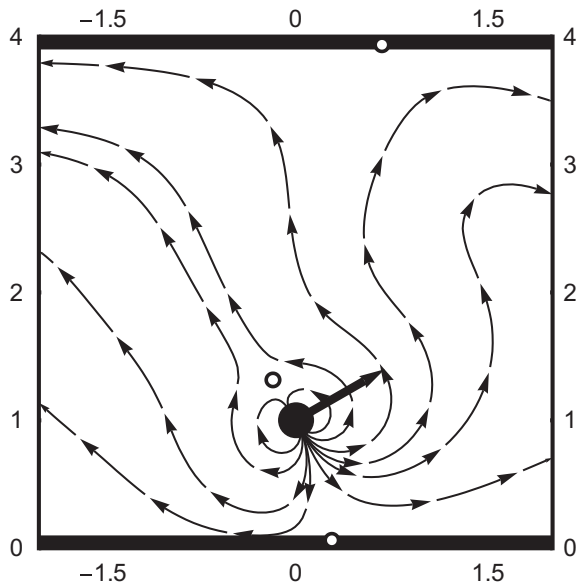


Figure 13. Shown are field lines for $\delta = 4$, $h = 1$ and $\gamma = \pi/3$. Tiny loops appear close to the dipole.

to the left of the dipole. Apparently, the system is very sensitive to small variations in parameters.

11. Locations of vortices and singularities

Energy flow patterns can become complicated, especially for a large separation δ between the mirrors, and details of the energy flow cannot always be resolved on the scale of the figure. For instance, in the flow pattern of Figure 14 there are 9 vortices and 11 singularities. At the centre of a vortex is a singular point. At such a point the Poynting vector σ is necessarily zero. This can be due to $e = 0$ or $b = 0$ or $e(\mathbf{r}) \times b(\mathbf{r})^*$ imaginary. For field points in the $\bar{y}\bar{z}$ plane, vector e is in the $\bar{y}\bar{z}$ plane. Since e is the complex amplitude, the condition $e = 0$ requires that the real and imaginary parts of both the \bar{y} and the \bar{z} components vanish simultaneously at a field point. Obviously, this is highly unlikely. The b vector, however, is along the \bar{x} axis, so $b = 0$ requires $\text{Re}b_x = 0$ and $\text{Im}b_x = 0$. Each equation defines a set of curves in the $\bar{y}\bar{z}$ plane, and at each intersection we have a singular point. In Figure 15, the solid lines are the solution of $\text{Re}b_x = 0$ and the dashed lines are the solution of $\text{Im}b_x = 0$. The parameters are $\delta = 8$, $h = 4$ and $\gamma = \pi/4$, which are the same as for the flow lines in Figure 10. The intersections of the curves, indicated by little black circles, appear to correspond to the locations of the four vortices in Figure 10. We have found in general that a singularity at the centre of a vortex is due to the vanishing of the magnetic field at that point.

Besides the centres of vortices, numerous other singularities appear and these are indicated by white circles in the figures. At such singularities, field lines split or collide,

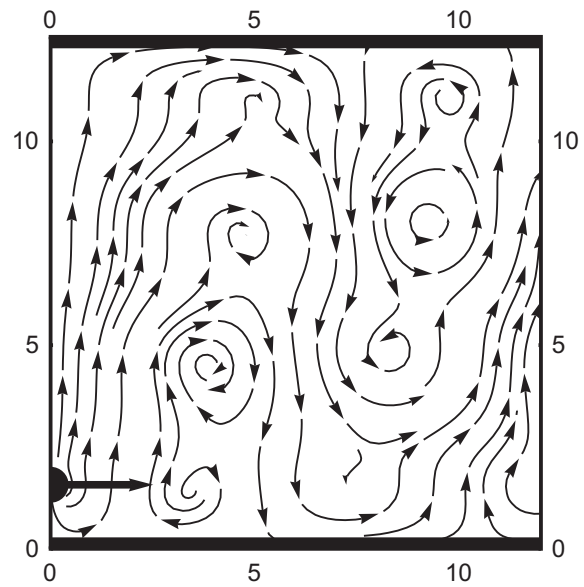


Figure 14. Shown are field lines for $\delta = 4\pi$, $h = \pi/2$ and $\gamma = \pi/2$. Many vortices appear, more or less along vertical lines.

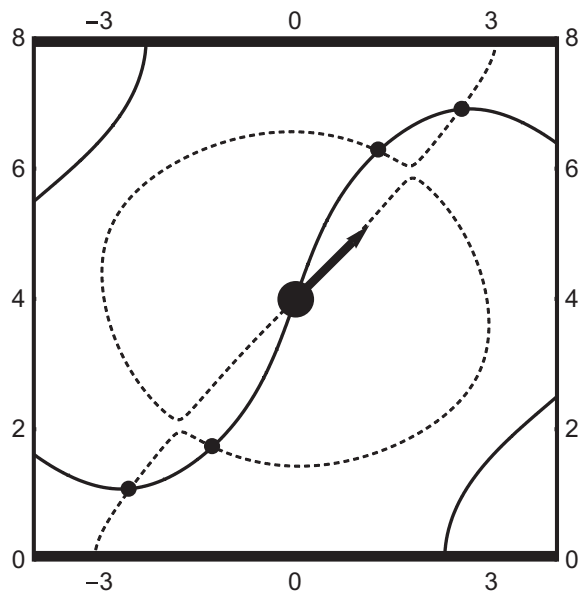


Figure 15. The solid lines are the solution of $\text{Re}b_x = 0$ and the dashed lines are the solution of $\text{Im}b_x = 0$ and the parameters are the same as for the field line pattern in Figure 10. The intersections, indicated by black circles, represent the locations of the four vortices.

as can be seen for instance in Figures 4, 11 and 13. Here, we have $e(\mathbf{r}) \times b(\mathbf{r})^*$ imaginary and this is the same as $\sigma = 0$. Since σ is in the $\bar{y}\bar{z}$ plane, this is therefore the same as $\sigma_y = 0$ and $\sigma_z = 0$. Both equations define sets of curves, and at the intersections the Poynting vector vanishes. Figure 16 shows these curves for the same parameters as in Figure 15. Interestingly, the condition $\sigma = 0$ includes the condition $b = 0$, so the black circles in Figure 16 are

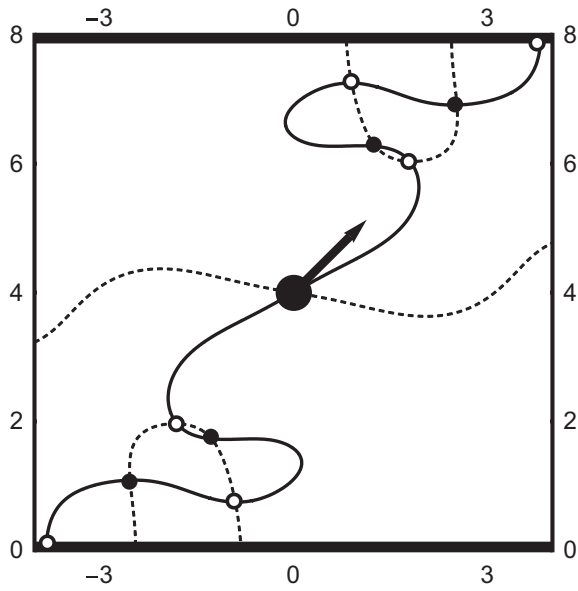


Figure 16. The solid lines are the solution of $\sigma_y = 0$ and the dashes lines are the solution of $\sigma_z = 0$ and the parameters are the same as for Figure 15. The black circles are the centres of vortices, and we conclude that by comparing to Figure 15. The white circles then must be singularities where field lines split.

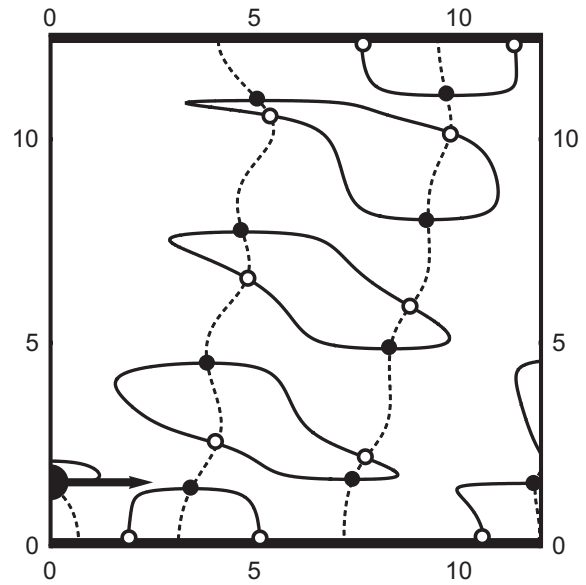


Figure 18. The intersections shown in the figure are the singularities of the energy flow diagram of Figure 14.

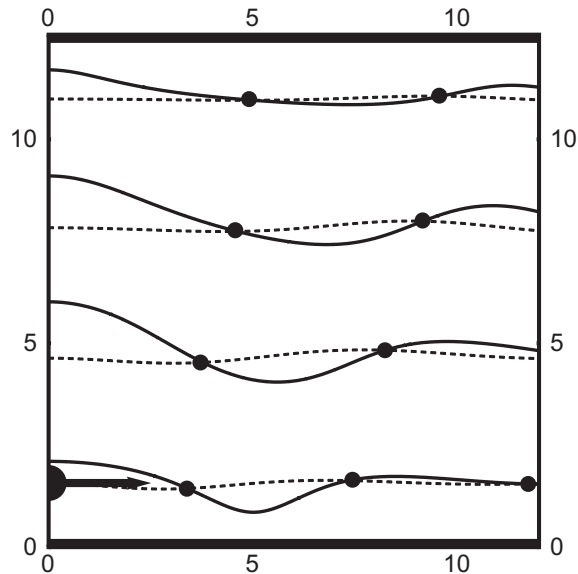


Figure 17. The solid and dashed lines represent the solutions of $\text{Re}b_x = 0$ and $\text{Im}b_x = 0$, respectively, for $\delta = 4\pi$, $h = \pi/2$ and $\gamma = \pi/2$. This corresponds to the flow line pattern of Figure 14.

at the same locations as the black circles in Figure 15. The sets of curves in both figures are very different, but they intersect at the same points for the locations of the vortices. In this fashion, we can tell which intersections in Figure 16 correspond to vortices and which intersections correspond to other singularities. Near a mirror surface, the Poynting vector is parallel to the mirror and so $\sigma_z = 0$.

Therefore, each mirror in the figure has a dashed line on top of it. Consequently, if a solid curve ends at a mirror, there is a singularity at this point. Two of these can be seen in Figure 16.

As another example, Figure 17 shows the solution of $\mathbf{b} = 0$ for $\delta = 4\pi$, $h = \pi/2$ and $\gamma = \pi/2$, and these are the same parameters as for the flow line picture of Figure 14. We see two sets of four vortices, more or less along upward lines. The one in the bottom-right corner is the lowest one of another set of four. Figure 18 shows the corresponding diagram for $\sigma = 0$. We notice 11 singularities, other than the 9 vortices. The locations of the vortices and singularities can very clearly be seen from Figure 18, whereas in the flow line picture of Figure 14, most of these locations are not clear at all.

12. Conclusions

The energy flow patterns for the propagation of electric dipole radiation in between parallel mirrors are far from trivial. The system only has three parameters: the dimensionless distance δ separating the mirrors, the dimensionless distance h between the location of the dipole and the lower mirror and the angle γ between the oscillation direction of the dipole moment and the normal to the mirror surfaces. For a radiating dipole in free space, most radiation is emitted perpendicular to the dipole axis (oscillation direction of the dipole moment) and none is emitted along the dipole axis. For a vertical dipole, as illustrated in Figure 3, this appears also to be the case for a radiating dipole in between mirrors, except that near the mirror surfaces the field lines of energy flow bend and

become parallel to the surfaces. This has to be so, since no radiation can penetrate the mirrors. When we look further away from the dipole, however, as in Figures 4 and 5, singularities appear. First, two singularities appear near the midway line between the mirrors and, further out, two singularities appear near the mirror surfaces. This pattern repeats indefinitely going outwards. In the figures, we use dimensionless coordinates for which 2π corresponds to an optical wavelength. Therefore, the pattern here, and in the following figures, are of near-wavelength or sub-wavelength scale.

For a horizontal dipole and small mirror separation we find again that most radiation is emitted perpendicular to the dipole axis and that the flow lines curve when they approach the mirrors, as shown in Figure 6. When the distance between the mirrors is increased, optical vortices appear in the vicinity of the dipole, as shown in Figure 8. When the dipole oscillates under a finite angle with the vertical, energy swirls around the dipole before taking off to infinity, as shown in Figure 9. For a larger separation between the mirrors we see from Figure 10 that several vortices appear in the flow pattern. Obviously, energy cannot accumulate at the centre of a vortex and cannot come out of the singularity at the centre of a vortex. It is shown in Figure 12 that the vortices in the plane of oscillation of the dipole should be seen as the cross sections of 3D vortices. Only in this plane is there a singularity at the centre of the vortex. When the dipole is located off-centre with the midpoint between the mirrors, small loops appear near the dipole. Field lines come out of the dipole at one side and then return back to the dipole at the other side. For larger separations between the mirrors, numerous vortices appear in the flow pattern of an off-centred dipole.

When flow patterns become complicated, an alternative way to look at these patterns is by considering the locations of the vortices and singularities, without reference to the flow lines. At the singularity at the centre of a vortex the magnetic field vanishes. This condition leads to two sets of curves and the vortices are located at the intersections. Typical examples are shown in Figures 15 and 17. Then, at any singularity the Poynting vector is zero and this condition also leads to two sets of curves. Any singularity is located at intersections in these diagrams. Since the singularities at the centres of the vortices

are also reproduced, we have a means of distinguishing between vortices and points where the singularities are due to the splitting of field lines. Examples are shown in Figures 16 and 18, with the black circles indicating the locations of vortices and the white circles represent any other singularities.

Disclosure statement

No potential conflict of interest was reported by the authors.

References

- (1) Novotny, L.; Hecht, B. *Principles of Nano-Optics*; Cambridge University Press: Cambridge, **2007**; Sections 8.3.3 and 10.5.
- (2) Morawitz, H. *Phys. Rev.* **1969**, *187*, 1792–1796.
- (3) Drexhage, K.H. *Prog. Opt.* **1974**, *XII*, 163–232.
- (4) Lukosz, W.; Kunz, R.E. *Opt. Commun.* **1977**, *20*, 195–199.
- (5) Lukosz, W.; Kunz, R.E. *J. Opt. Soc. Am.* **1977**, *67*, 1607–1615.
- (6) Chance, R.R.; Prock, A.; Silbey, R. *Adv. Chem. Phys.* **1978**, *39*, 1–65.
- (7) Sipe, J.E. *Surface Sci.* **1981**, *105*, 489–504.
- (8) Ford, G.W.; Weber, W.H. *Surface Sci.* **1981**, *105*, 451–481.
- (9) Ford, G.W.; Weber, W.H. *Phys. Rep.* **1984**, *113*, 195–287.
- (10) Novotny, L. *J. Opt. Soc. Am. A* **1997**, *14*, 91–104.
- (11) Lukosz, W.; Kunz, R.E. *J. Opt. Soc. Am.* **1977**, *67*, 1615–1619.
- (12) Arnoldus, H.F.; Foley, J.T. *J. Opt. Soc. Am. A* **2004**, *21*, 1109–1117.
- (13) Philpott, M.R. *Chem. Phys. Lett.* **1973**, *19*, 435–439.
- (14) Milonni, P.W.; Knight, P.L. *Opt. Commun.* **1973**, *9*, 119–122.
- (15) Chance, R.R.; Prock, A.; Silbey, R. *J. Chem. Phys.* **1974**, *60*, 2744–2748.
- (16) Chance, R.R.; Miller, A.H.; Prock, A.; Silbey, R. *Chem. Phys. Lett.* **1975**, *33*, 590–592.
- (17) Chance, R.R.; Prock, A.; Silbey, R. *J. Chem. Phys.* **1975**, *62*, 771–772. Misprints in Equations (1), (10) and (11).
- (18) Nha, H.; Jhe, W. *Phys. Rev. A* **1996**, *54*, 3505–3513.
- (19) Hulet, R.G.; Hilfer, E.S.; Kleppner, D. *Phys. Rev. Lett.* **1985**, *55*, 2137–2140.
- (20) Li, X.; Arnoldus, H.F. *Phys. Rev. A* **2010**, *81*, 053844-1-10.
- (21) Li, X.; Arnoldus, H.F. *Opt. Commun.* **2013**, *305*, 76–81.
- (22) Arnoldus, H.F.; Berg, M.J.; Li, X. *Phys. Lett. A* **2014**, *378*, 755–759.
- (23) Arnoldus, H.F.; Berg, M.J. *J. Mod. Opt.* **2015**, *62*, 244–254.
- (24) Jackson, J.D. *Classical Electrodynamics*, 3rd ed.; Wiley: New York, NY, **1999**; p 411.